Study on an Ideal Elastic Deformation of Flapping Wing Due to Some Ribs by Finite Element Method

Junchangpood A[1], Fuchiwaki M[1*] and Tanaka K[2,*]

[1] Department of Mechanical Information Science and Technology
Kyushu Institute of Technology, 680-4 Kawazu, Iizuka, Fukuoka, 820-8502
[1*]Corresponding Author: futiwaki@mse.kyutech.ac.jp, +81 948 29 7783, +81 948 29 7751
[2*]Corresponding Author: kazuhiro@mse.kyutech.ac.jp, +81 948 29 7773, +81 948 29 7751

Abstract

In this paper, we present the structural deformations, which will be highlight the information of an ideal elastic deformation for development the fluid applications in future. The flying insects, birds, and aquatic animals fly and swim skillfully by controlling a flow field around their body using their wings or tail flukes of complex shape and their elastic deformation. Since. the insect have been evolved and perfected their flight, making them the most agile and maneuverable creatures for their size today. Hence, many researchers attempt to mimic these characteristics of the insect flight, and construct a small flapping robot or MAVs for performing the special missions. However, the flow field around the moving elastic body is treated as a coupled problem of fluids and structures (Fluid Structure Interaction Problem, FSI). Furthermore, there are a variety of the phenomena with applications in many areas. The flying robot is only one of the applications on the fluid-structure combination working. For solving FSI problems, 3-D structural deformations largely and complexly have been very difficult to resolving these deformation with making the structural function deforming. Hence, We were going to carry out the elastic deformations of the wing structures by the finite element method (FEM). In addition, we varied a simple wing structures with three cases of the wing structures. In the analysis of the flow around flapping rigid wing, we found, that the butterfly robot obtain lift by flapping wings, caused to making vortices also, and a pair of large-scale vortices is formed on the wing tip. Lift and Drag are changed with the flapping wing position very well. Moreover, in the case of structural analysis, some ribs included with main spar on the wing structures could control the wing deformation. In particular, the maximum deformation occurs at the trailing edge on the membrane.

Keywords*:* Finite Element Method, Flapping Elastic Wing, Structural Flexibility, Wing Deformations.

1. Introduction

Flying insects, birds, or aquatic animals fly or swim skillfully by controlling a flow field around their body using their wings or tail flukes of complex shape and their elastic deformation. There are two classes of aerial flapping flight

(insect-like and bird-like). Birds have the muscles attached to bones along the wing, used for flight and maneuvering. This makes them heavy and relatively less efficient (in terms of specific power). On the other hand, insects possess an exoskeleton: all actuation is carried out at the wing root and, consequently, the wing structure is very light, generally accounting for ~1% of the insect's weight. This makes insect flight very attractive as a model, while also satisfying all the other requirements of the flight envelope identified above (especially hover) for the micro air vehicles (MAVs) [1-2]. Hence, the insect have been evolved and perfected their flight, making them the most agile and maneuverable creatures for their size today. Many researchers attempt to mimic these characteristics of the insect flight, and construct a small flying robot or MAVs for performing the special missions[2-9]. It is conceived, that flying insects acquire lift through interaction with the vortex around the wing boundary generated by flapping, and therefore, many researchers have recently been studied on this mechanism by the way of the experiment numerical analysis before[5-11]. Furthermore, there are a variety of the phenomena with applications in many areas, such as, analysis of aneurysms in large arteries, stability analysis of the aircraft wings, turbomachinery design, design of the bridges, and so on. This is a new challenges in the fluid engineering field to clearly understand the phenomena of deforming structure largely and complexly associated a flow field characteristics. Presently, other researchers have investigated the flexibility effects on the aerodynamics of flapping wing by the experiments only in large wing[12-14], and 2D-simulation[15]. However, this information can also be used for solving the fluid-structure coupled problems, needed for the engineering design of the ornithopters. These problems become even more difficult and highly complex, when the deformation of the elastic body by a fluid is introduced and flow field varies with the moving body. However, it has not been fully solved. Presently, we have been investigating on a flow field around a flapping robot wing, which is one of fluid-structure interaction (FSI) applications as mentioned before. In our previous works, we have performed about a flow field around the flapping rigid wings through numerical analysis. In this work, one-way coupled analysis was employed for considering a moving boundary problems, in which the elastic deformation is expressed by a function[11]. In the case of the flapping rigid wing or small deformation, the way of giving a structural deforming functions have performed the wing deformation accurately. On the other hand, other researchers proposed the method of the finite element model to consider the structural deformations, in the cases of small deformation mostly[16-18]. However, in the case of a large and complex deformation, it could not be probably resolved by the functions. Hence, we have been going to resolve this structural problem with the finite element method (FEM). In present work, to determine a ideal elastic deformation of the wing structures due to some ribs, three types of the wing structure were varied for modeling as shown in Fig. 1. The elastic deformations were obtained for different

wing structures and materials, and we show how the elastic deformation and inertial flapping

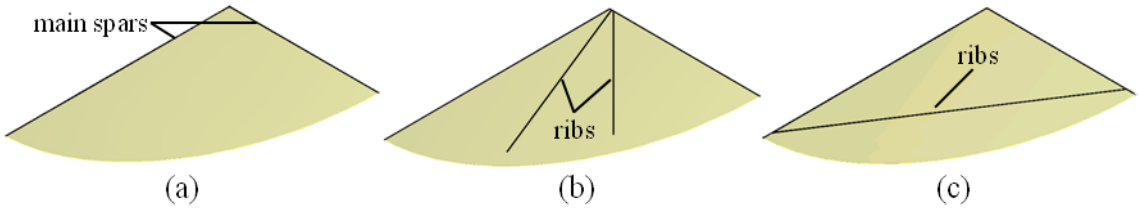

Fig. 1 Wing structures for structural analysis, (a) A-Type, (b) B-Type, (c) C-Type

forces affect the dynamical behavior of the flapping wings.

2. Theories

The numerical analysis divided between the computational fluid dynamics(CFD) and computational solid dynamic(CSD) are described

2.1 Fluid dynamic analysis

For analysis of the flow phenomena, a flow over the flapping rigid wing is considered. The governing equations and assumptions are the unsteady flow, three-dimensional incompressible, and turbulent flow. Hence, the continuity and Navier-Stokes equation [19] can be given a Eqs. (1) and (2).

$$\frac{\partial \rho}{\partial t}+\frac{\partial}{\partial x_i}\left(\rho u_i\right)=0 \qquad (1)$$

$$\frac{\partial}{\partial t}\left(\rho u_i\right)+\frac{\partial}{\partial x_j}\left(\rho u_i u_j\right)=-\frac{\partial p}{\partial x_i}+$$

$$\frac{\partial}{\partial x_j}\left[\mu\left(\frac{\partial u_i}{\partial x_j}+\frac{\partial u_j}{\partial x_i}-\frac{2}{3}\delta_{ij}\frac{\partial u_l}{\partial x_l}\right)\right]+\frac{\partial}{\partial x_j}\left(-\rho\overline{u_i' u_j'}\right) \qquad (2)$$

Here, u is the velocity, P is the pressure, ρ is the density of air, and μ is the viscosity.

In a turbulent flow, due to the flow behaviors around the flapping robot are the turbulent flows, therefore a turbulent modeling is considered also. The modified equations contain additional unknown variables, and turbulent models are needed to determine these variables in the terms of know quantities. In this simulation model, Shear-Stress transport(SST) $k-\omega$ model [20-22] was chosen, because the $k-\omega$ model can predict a characteristic behavior well in the boundary layer on the wings. The transport equations for SST $k-\omega$ model are the turbulence kinetic energy (k) and specific dissipation rate (ω), which are given as Eq. (3) and (4);

The turbulence kinetic energy (k):

$$\frac{\partial(\rho k)}{\partial t}+\frac{\partial(\rho k u_i)}{\partial x_i}=\frac{\partial}{\partial x_j}\left(\Gamma_k\frac{\partial k}{\partial x_j}\right)+G_k-Y_k+S_k \qquad (3)$$

The specific dissipation rate (ω):

$$\frac{\partial(\rho\omega)}{\partial t}+\frac{\partial(\rho\omega u_i)}{\partial x_i}=\frac{\partial}{\partial x_j}\left(\Gamma_\omega\frac{\partial \omega}{\partial x_j}\right)+G_\omega-Y_\omega+S_\omega \qquad (4)$$

In Eq. (3) and (4), the G_k represents the generation of turbulence kinetic energy due to mean velocity gradients. The G_ω represents the generation of specific dissipation rate. The Γ_k and Γ_ω represent the effective diffusivity of k and ω, respectively. The Y_k and Y_ω represent the dissipation of k and ω due to turbulence. The S_k and S_ω are user defined source terms. All of the above terms are calculated as described in reference [20] .

2.2. Structural Analysis

When the flapping elastic wing is working, is treated as a transient structural problem. To determine the time-varying displacements, strain or internal forces, we have also concerned over the structural behavior of the flapping elastic wing under an inertia force. In continuum mechanics, the equations of

motion, that govern the structural dynamics of the flapping elastic wing can be given as Eq. (5).

$$[M]\{\ddot{q}(t)\}+[C]\{\dot{q}(t)\}+[K]\{q(t)\}=\{R(t)\} \quad (5)$$

Where $R(t)$ is a vector containing the aerodynamic forces associated with the aerodynamic loads, and $\{\ddot{q}(t)\}$, $\{\dot{q}(t)\}$, and $\{q(t)\}$ are the acceleration, velocity and displacement vectors of the finite element assembly, respectively. These governing equations are solved by the discretization method being the finite element method (FEM) [23].

3.2. Kinematic motion of flapping robot's wing

For the kinematics equation of flapping robot's wings, a time-varying flapping angle is defined by Eq. (6) referred with the paper[11].

$$\theta=[A]\sin(2\pi f(t+t_0)+\varphi)-\theta_0 \quad (6)$$

Where, A is the flapping amplitude (20 degree), f is the flapping frequency (about 10 Hz), t_0 is the initial time of flapping (about 0.01128 sec.), φ is the phase different angle (π rad), and θ_0 is the initial angular position (about 12.4 degree). The flapping angle as Eq. (6) was defined for boundary conditions both of fluid modeling and structural modeling. In the fluid modeling, the wall boundary condition was defined as moving boundary condition with Eq. (6). Also, in the structural modeling, the support condition was defined by the remote displacement with Eq. (6).

3. Materials and Methodology

In this class of methodology, the flow field around the flapping rigid wing is performed with FLUENT 6.3, and the deformation behavior is carried out by ANSYS FE 12.1.

3.1 Flapping robot's wing

The both flapping rigid wing used in the fluid dynamic analysis and the flapping elastic wing used in the structural analysis, are same dimension with a real flying robot wing in experiment. The wing structures are defined as the main spars part and the membrane part, which the main spar is the carbon rod material and the membrane is the special paper as shown in Fig. 2. The haft wingspan(Ls) and chord length(c) are 120 and 80 cm, respectively.

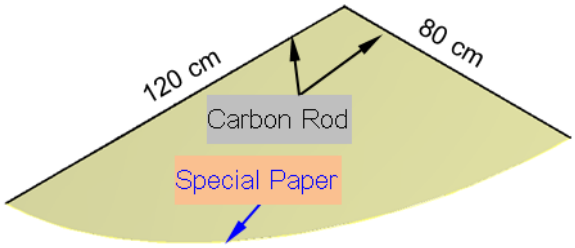

Fig.2 Wing Structures in Structural Analysis

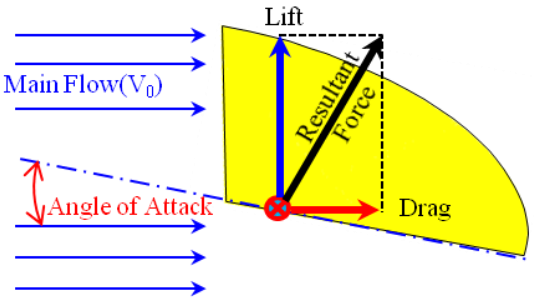

Fig.3 Angle of Attack defined in Flow Analysis

3.2 Numerical method

In the fluid dynamic analysis, the vortex structures and unsteady aerodynamic characteristic were considered with varying the angles of attack as 0, 5 and 10 degree as shown in Fig.3. the fluid analysis domain and boundary conditions shown in Fig. 4(a), which is the front, the back, the span length, and the length in vertical direction are given to 2c, 5c, 3c, and 2c, respectively. In simulation, the dynamic mesh method is provided for solving a moving boundary problem. In addition, the mesh type of hexahedral cells are needed for this method, which the mesh at near robot wings

zone is shown in Fig. 4(b). The fluid analysis conditions are defined as shown in Table. 1.

In the part of structural analysis. The flexible wings used in the nonlinear elastic model are also varied with Young's modulus and density in three cases as shown in Table. 2. Due to the true material properties used to constructing the wing structure are not measured, then it were defined by referring with the material property region of the carbon rod and paper. Figure 6 shows the computational grid of wing structure, and the conditions in structural analysis are defined as shown in Table. 3.

4. Results and Discussions

4.1 Vortex structure around flapping rigid wings

We captured the flow field around the robot's wings while it were flapping. Therefore, the vortex structure varied with the flapping wing positions was explained by the vorticity contours as shown in Fig. 7. This is the iso-surface vorticity of 160 1/s around flapping rigid wing varying, which the wing positions following this are: the top-dead point, moving down-center point, bottom-dead point, and moving up-center point, as shown in Figs. 7(a) – 7(d), respectively. We found, that the high velocities occur at tip-wing and trailing edge, because these positions had the high momentum transfer from the edge of the wing to the wake structure behind the wings. Moreover, the vorticity were largest behind tailing edge and near tip-wings, because difference between velocity gradient in X and Y axis, has been large and growth up from body to tip-wings. The vortices behind the wings are generated by flapping wings, which it could be indicated the behaviors of rotation fluid flow.

Furthermore, we also obtained the time-varying of the drag and lift coefficient as shown in Figs. 8(a) and 8(b), respectively. It show, both drag and lift are similar tendency for other angles of attack. It is demonstrated, that the body attack angle was affected to the drag

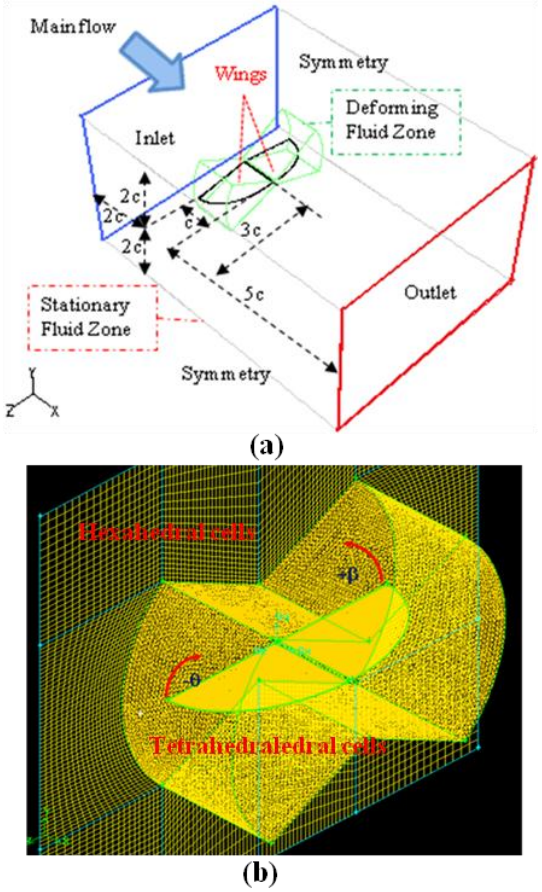

Fig. 4 Fluid analysis domain, (a) boundary conditions. (b) computational grid around the flapping rigid wing

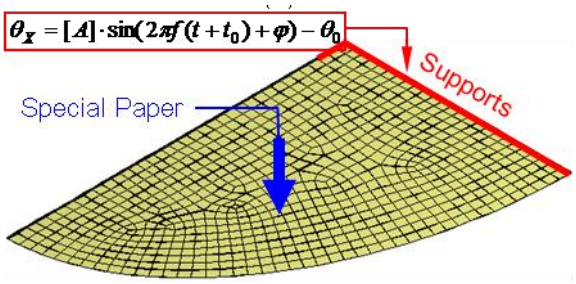

Fig.6 Computational grid and Boundary conditions in Structural modeling

coefficient very well, as shown in Fig. 8(a). In addition, it depends on the flapping angle position. Hence, It is shown, that the unsteady drag force on the robot's wings occurs, when it is flying by flapping. In the term of the lift coefficient, it increases lightly with increasing the attack angle, and also has similar tendency with drag behavior, as shown in Fig.8(b).

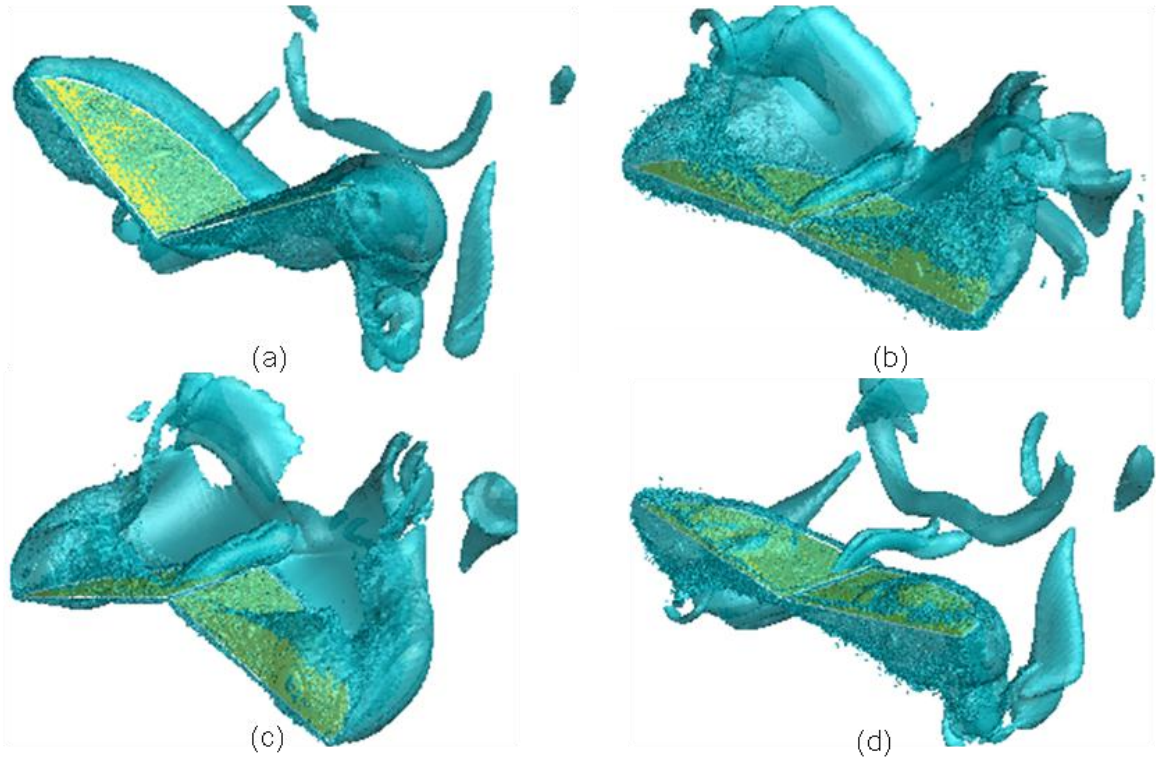

Fig. 7 Vorticity around flapping rigid wing varying the wing positions, (a) Top-dead point, (b) Moving down-center point, (c) bottom-dead point, (d) Moving up-center point

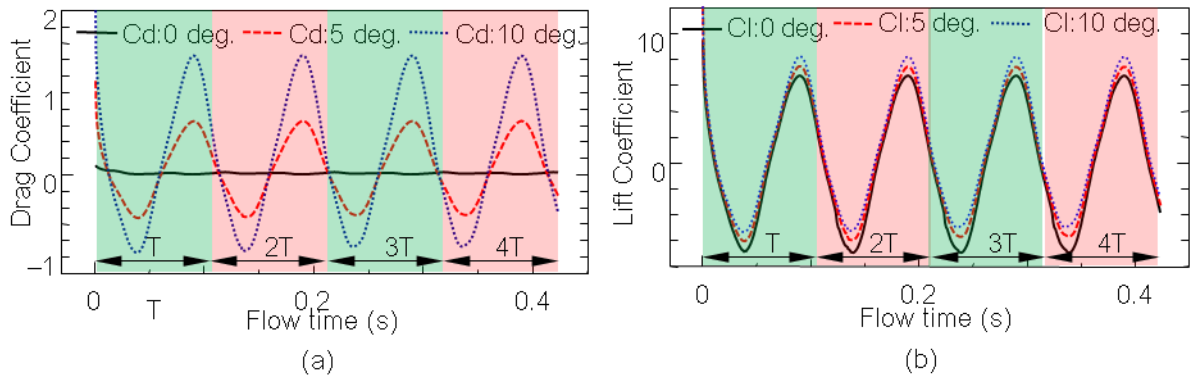

Fig. 8 unsteady aerodynamic characteristics, (a) drag coefficient, (b) lift coefficient

4.2 Wing deformations

In the results of structural analysis, the wing deformations were evaluated in three types of wing structures as shown in Fig. 9. The contours of the elastic deformations on the wing structures are plotted, in order to clearly show the elastic deformation variations. The key feature observed here is the presence of two regions of the deformations, that rapidly change as the wing positions. The results demonstrated

the deformations of A-Type, B-type, and C-Type wings at the top-dead and bottom-dead points with Young's modulus of the carbon rod of 133 MPa as shown in Figs. 9(a) and 9(b), respectively. As is shown in Figures, the elastic deformation strongly depends on the positions of flapping angles. In addition, the elastic deformations depend on the structural flexibility (*E*) very well as shown in Fig. 10. Each wing structures are fixed the global second moment of area(*I*) by using the same dimension of wing structure. Moreover, we found, that not only the deformations on the main spar is decreased, but also the deformation on the membrane at the trailing edge. Due to an influence of the main spar strength at trailing edge reinforces on the membrane, hence the deformation is decreased either. Also, the simulation results show, that the maximum deformation occur following this, 15, 9, and 7 mm with Young's modulus as 133, 350, and 533 MPa. as shown in Figs. 10(a)-10(c),respectively. Furthermore, the positions and length of some ribs attached with the main spars are very strong effects with the deformation on the membrane, because the carbon rod connected with the membrane is high bending stiffness(*EI*). Hence, the maximum deformation is decreased by some ribs as comparison with the original wing (A-Type wing).

5. Conclusions

In the case of the analysis of the flow field around the flapping rigid wing, We found, that the flying robot obtains lift force by flapping wings, caused to making the vortices also. Moreover, a pair of large-scale vortices is formed on the wing tip.

In the structural analysis, we also found, that some spar attached with the main spar on the wing structures could control the wing deformations. In particular, the max-deformation occurs at the trailing edge on the membrane. We expect, that the results of the structural analysis will be the advantages with FSI analysis on the flow phenomena around the flapping elastic wings. In a future work, we will be going on the full FSI analysis to determine the good structural deformation generated the better flow around the flapping elastic wing by using the same wing model in the structural analysis.

Table. 1 Fluid simulation conditions

Fluid	Air	Inlet	1.5 [m/s]
Mesh	Hexa &Tetra	Outlet	0 [Pa]
Element number	3.e+06	Wall	Symmetry
Turbulence	SST k-w	Time step	1.e-04 [s]
Iteration	15	Flapping cycle	4
Re	8215	Cal. time	Two months

Table. 2 Material properties of wing structures

Materials	Young's modulus(E) [GPa]	Density [kg/m^3]	Poison's ratio
Carbon rod A	133	1400[13]	0.28
Carbon rod B	350	1500	0.3
Carbon rod C	533	1600	0.3
Special Paper	1.	300	0.3

Table. 3 Structural simulation conditions

Structure	Carbon Rod/ Special Paper	Analysis Type	Transient Structural
Stiffness Behavior	Flexible	Supports	Remote Displacement
Inertial	g_y=-9.806 m/s^2	Node number	3.e+04
Initial Velocity	0. m/s	Time step	1.e-04 [s]
Flapping cycle	4	Cal. time	4 day

6. References

[1] Shyy, W., Berg, M. and Ljungqvist, D. (1999). Flapping and flexible wings for biological and micro air vehicles, *Progress in Aerospace Sciences*, vol. 35(5), July 1999, pp. 455 – 505.

[2] Galinski, C. and Zbikowski, R. (2007), Materials challenges in the design of an insect-

like flapping wing mechanism based on a four-bar linkage, *Materials and Design,* vol.28(3), February 2006, pp. 783 - 796.

[3] Nguyen, Q.V., Truong, Q.T., Park, H.C., Goo, N.S. and Byuni, D. (2010), Measurement of Force Produced by an Insect-Mimicking Flapping-Wing System, *Journal of Bionic Engineering,* vol.7(supp1), September 2010, pp. S94 – S102.

[4] Tsai, B-.J. and Fu, Y-.C. (2009), Design and aerodynamic analysis of a flapping-wing micro aerial vehicle, *Aerospace Science and Technology,* vol.13(7), October-November 2009, pp. 383 - 392.

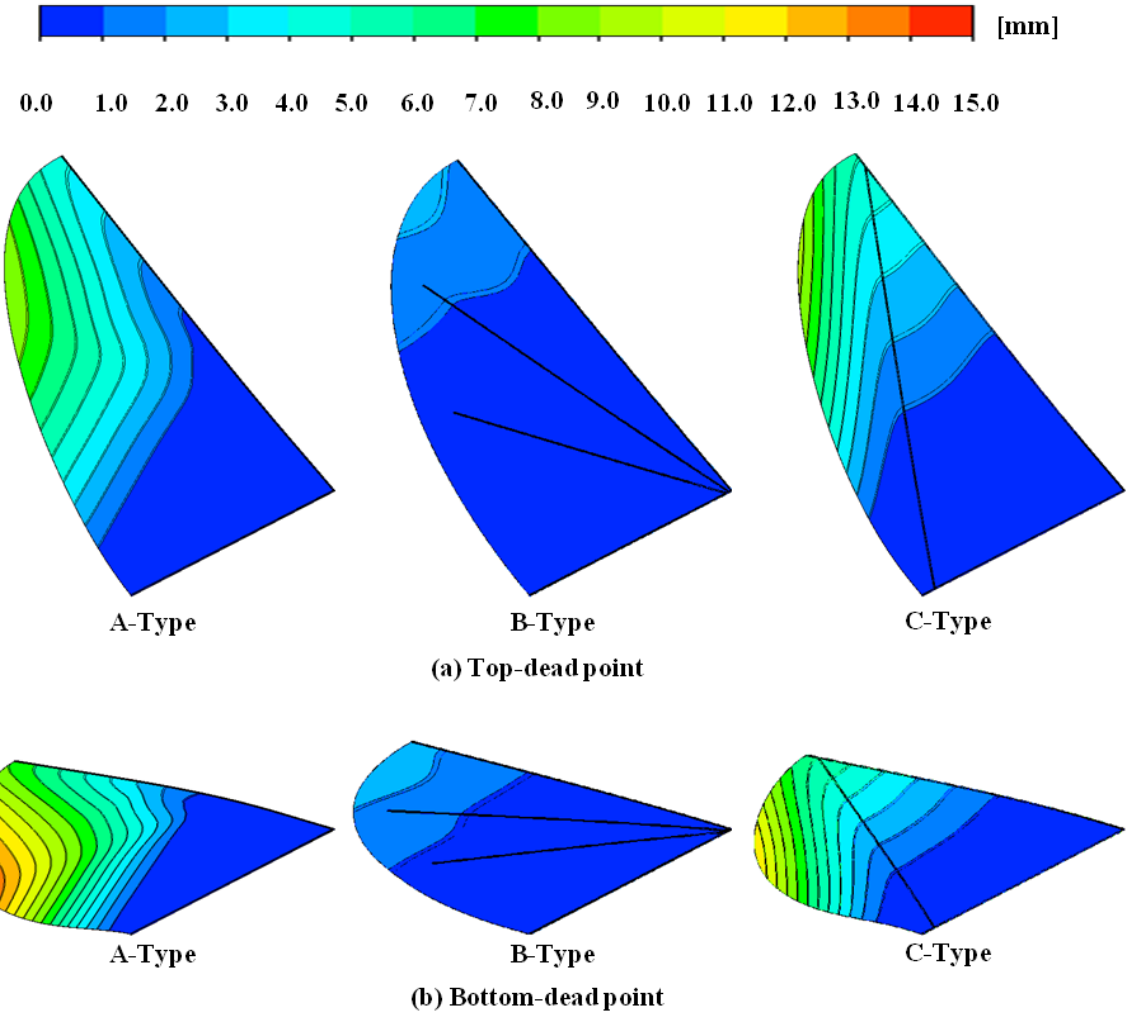

Fig. 9 Deformation as varying wing positions, (a) Top-dead point, (b) bottom-dead point

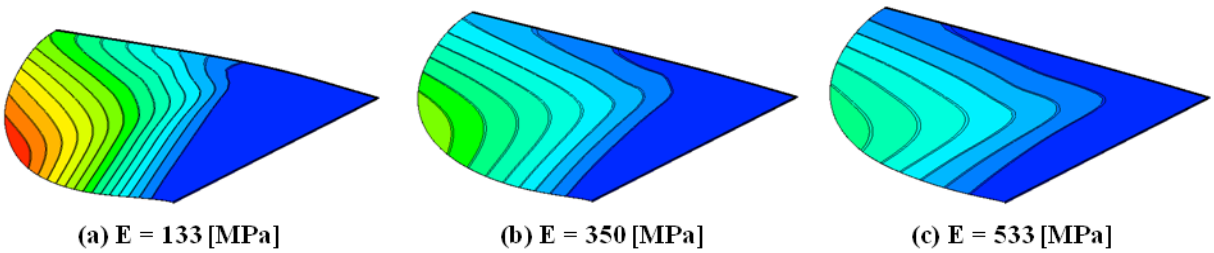

Fig. 10 Max-Deformation as varying Young's modulus, on A-Type wing

[5] Wang, Z.J. (2000). Vortex shedding and frequency selection in flapping flight. *Journal of Fluid Mechanics*, vol. 410(1), September 2000, pp. 323 - 341.

[6] Lian, Y., Shyy, W., Viieru, D. and Zhang, B. (2003). Membrane wing aerodynamics for micro air vehicles. *Progress in Aerospace Sciences*, vol. 39(6-7), August-October 2003, pp. 425 - 465.

[7] Von Ellenrieder, K.D., Parker, K. and Soria, J. (2008). Fluid mechanics of flapping wings. *Experimental Thermal and Fluid Science*, vol. 32(8), September 2008, pp. 1578 - 1589.

[8] Deng, X., Schenato, L. and Sastry, S. (2006). Flapping Flight fot Biomimetic Robotic Insects: Part II –Flight Control Design. *IEEE Transactions on Robotics*, vol. 22(4), June 2006, pp. 789 - 803.

[9] Fujikawa, T., Hirakawa, K., Okuma, S. and et al. (2008). Development of a small flapping robotMotion analysis during takeoff by numerical simulation and experiment, *Mechanical Systems and Signal Processing,* vol.22(6), August 2008, pp. 1304 - 1315.

[10] Zhang, Q. and Hisada, T. (2001). Analysis of fluid-structure interaction problems with structural buckling ang large domain changes by ALE finite element method, *Computer Method in Applied Mechanics and Engineering,* vol.190(48), September 2001, pp. 6341 - 6357.

[11] Junchangpood, A., Fuchiwaki, M. and Tanaka, K. (2010). Study on vortex Structure and Dynamic Forces on Flapping Wings of Small Flying Robot by Numerical Simulation, paper presented in *the 10th Global Congress on Manufacturing and Management(GCMM2010) 2010*, Bangkok, Thailand.

[12] Combes, S.A. and Daniel, T.L. (2003). Into thin air: contributions of aerodynamic and inertial-elastic forces to wing bending in the hawkmoth *Manduca sexta*, *The Journal of Experimental Biology*, vol. 206(1), September 2003, pp. 2999 – 3006.

[13] Mazaheri, K. and Ebrahimi, A. (2010). Experimental investigation of the effect of chordwise flexibility on the aerodynamics of flapping wings in hovering flight, *Journal of Fluids and Structures*, vol. 26(4), May 2010, pp. 544 – 558.

[14] Heathcote, S., Wang, Z. and Gursul, I. (2008). Effect of spanwise flexibility on flapping wing propulsion, *Journal of Fluids and Structures*, vol. 24(2), February 2008, pp. 183 – 199.

[15] Le, T.Q, Ko, J.H., Byun, D., Park, S.H. and Park, H.C. (2010). Effect of Chord Flexure on Aerodynamic Performance of a Flapping Wing, *Journal of Bionic Engineering*, vol. 7(1), March 2010, pp. 87 – 94.

[16] Jin, T., Goo, N.S. and Park, H.C. (2010), Finite Element Modeling of a Beetle Wing, *Journal of Bionic Engineering,* vol.7(supp1), September 2010, pp. S145 – S149.

[17] Combes, S.A., Daniel, T.L. (2003). Flexual stiffness in insect wings I, Scaling and the influence of wing venation, *Experimental Biology*, vol. 206, June 2003, pp. 2979 – 2987.

[18] Combes, S.A., Daniel, T.L. (2003). Flexual stiffness in insect wings II, Spatial distribution and dynamic wing bending, *Experimental Biology*, vol. 206, June 2003, pp. 2989 – 2997.

[19] Hoffmann, K.A., and Chiang, S.T. (2000).

Computaional Fluid Dynamics III. 4th ed., Engineering Education System, Wichita Kan.

[20] Wilcox, D. C. (1998). Turbulence Modeling for CFD, DCW Industries, Inc., La Canada, California.

[21] Menter, F. R., Kuntz, M. and Langtry, R. (2003). Ten Years of Experience with the SST Turbulence Model. In K. Hanjalic, Y. Nagano, and M. Tummers, editors, Turbulence, Heat and Mass Transfer 4, Begell House Inc., 625-632.

[22] Menter, F.R. (1994). Two-Equation Eddy-Viscosity Turbulence Models for Engineering Applications. *AIAA Journal*, vol.32(8), August 1994, pp. 1598 - 1605.

[23] Sugiyama, K. and Sumoto, Y., (2011). A full Eulerian finite difference approach for solving fluid-structure coupling problems. *Journal of Computational Physics*, vol. 230(3), Febuary 2011, pp. 596 - 627.